Detecting unstable periodic orbits in chaotic time series using synchronization

Ali Azimi Olyaei and Christine Wu
Department of Mechanical and Manufacturing Engineering, University of Manitoba, Winnipeg, Manitoba, R3T 5V6 Canada

Witold Kinsner
Department of Electrical and Computer Engineering, University of Manitoba, Winnipeg, Manitoba, R3T 5V6 Canada
(Received 17 February 2017; revised manuscript received 23 May 2017; published 12 July 2017)

An alternative approach of detecting unstable periodic orbits in chaotic time series is proposed using synchronization techniques. A master-slave synchronization scheme is developed, in which the chaotic system drives a system of harmonic oscillators through a proper coupling condition. The proposed scheme is designed so that the power of the coupling signal exhibits notches that drop to zero once the system approaches an unstable orbit yielding an explicit indication of the presence of a periodic motion. The results shows that the proposed approach is particularly suitable in practical situations, where the time series is short and noisy, or it is obtained from high-dimensional chaotic systems.

DOI: 10.1103/PhysRevE.96.012207

I. INTRODUCTION

Unstable periodic orbits (UPOs) embedded in chaotic attractors play a fundamental role in understanding chaotic dynamics. The presence of such orbits in experimental data is an evidence of determinism. It is an important concept that defines several properties of chaotic attractors such as Lyapunove exponents, fractal dimensions, and topological entropy [1]. Identification of UPOs within chaotic attractors is also important from a practical point of view. It reveals essential information required in many practical situations such as noise reduction [2], control [3], chaotic communication [4], and chaotic computing [5]. Therefore, investigation of UPOs embedded in chaotic attractors is important to understand and exploit the underlying dynamics.

Detecting UPOs from experimental data has been addressed in the past, and various methods have been proposed. The classical methods utilize the recurrence properties of chaotic attractors in the full state space [6], or on a Poincaré section [7]. They follow the evolution of the trajectory, and record the moment at which the trajectory returns to a small neighborhood of some recurrent point. The statistical analysis is then conducted to determine whether the recurrent point belongs to a UPO, or to improve the initial estimation of it. More recent methods propose a different approach. They suggest utilizing advanced techniques such as neural network [8], directed weighted complex network [9], or Kalman filters [10] to estimate the vector field of the underlying dynamics, through which UPOs can be extracted. In a different approach, an estimated symbolic model and the classical graph theory has been used to extract UPOs [11]. An important building block of the previously proposed methods is reconstruction of the state space trajectories form a single time history of the system [12]. Note that the reconstruction of the state space trajectory is not a trivial task considering that only a short and noisy time series is available in many practical situations. Moreover, identifying a Poincaré section, or estimating the vector field of the underlying system can be complicated by the fact that no analytical knowledge of the system is available in many practical situations.

This paper proposes a different approach using the concept of synchronization to detect UPOs in experimental chaotic time series. It is based on a synchronization problem in which the chaotic system drives a system of harmonic oscillators through a proper coupling condition. The synchronization scheme is designed so that the power of the coupling signal exhibits notches that drop to zero at the vicinity of UPOs. In contrast to the previous methods, this approach does not require either state space reconstruction, or an estimation of the vector field of the underlying dynamics. It detects UPOs by simply looking at the notches in the power of the coupling signal. The success of the proposed approach is demonstrated by detecting UPOs embedded in chaotic time series obtained from numerical simulations of the well-known Rössler system, and Mackey-Glass equation. The results show that the proposed method leads to accurate results even if the time series is short and noisy, or it is obtained from high-dimensional chaotic systems.

II. METHODOLOGY

This paper develops an algorithm of detecting UPOs embedded in a chaotic time series using a synchronization problem described by

$$\dot{a}_n = in\omega a_n + \kappa_n\left(y - \sum_{r=-\infty}^{\infty} a_r\right), \tag{1}$$

where a_n is a component of the synchronized system for $n \in \mathbb{Z}$, y is a scalar output of the chaotic system, ω is the angular frequency parameter, κ_n is the coupling strength such that κ_n is the complex conjugate of κ_{-n}, and $i^2 = -1$. Equation (1) defines an external synchronization problem in which the chaotic system drives a system of harmonic oscillators $\dot{a}_n = in\omega a_n$ through the coupling $f = y - \sum_{r=-\infty}^{\infty} a_r$ of the gain κ_n. The coupling gains are assigned so that the synchronized system remains bounded, and forgets its initial condition as $t \to \infty$ [13]. Note that the synchronization problem described by Eq. (1) is a unidirectional version of the synchronization scheme proposed in [13]. However, it has different characteristics. The synchronization problem proposed in [13] presents a bidirectional coupling that describes mutual interactions between the chaotic system and the system of harmonic oscillators. It aims to stabilize a target unstable orbit by assuming ω is a known parameter identical to the frequency of the target orbit. This paper proposes a synchronization scheme, in which the chaotic system affects the behavior of the harmonic oscillators, while the reverse does not happen. Since the chaotic system remains intact, y can play the role of a recorded time history. Moreover, it assumes that ω is a variable parameter, and detects the coordinates of the UPOs embedded in the chaotic signal by studying the response of the synchronized system with respect to the frequency parameter. The relation between the extended delayed feedback control (EDFC) [14] and the bidirectional version of the proposed coupling scheme of this paper for $\kappa_n = \kappa$ has been investigated in [15]. It has been shown that both schemes have identical spectral properties when dealing with periodic signals provided that the delay in the feedback loop of EDFC and the period of harmonics oscillators $\frac{2\pi}{\omega}$ are set to be equal. This observation leads to a simple method of evaluating linear stability properties of EDFC controlled orbits. However, this work is of a different nature, as it deals with chaotic signals characterized by continuous frequency bandwidths. It tries to find the frequency parameter and the moment of time that correspond to an unstable periodic motion by analyzing a unidirectionally coupled version of the synchronization scheme. While [15] is concerned with evaluating linear stability properties of EDFC controlled orbits (Floquet exponents), this paper aims to extract nonlinear features of chaotic attractors (UPOs).

The proposed approach detects UPOs embedded in chaotic time series by examining the periodicity of the system of coupled harmonic oscillators as described by Eq. (1). It is based on a weak formulation of the synchronized system with respect to a set of orthogonal test functions $\{e^{im\omega(t-\tau)}\}_{m=-\infty}^{\infty}$, which is defined in the interval of interest $\tau < t < \tau + \frac{2\pi}{\omega}$, as described by

$$\int_{\tau}^{\tau+\frac{2\pi}{\omega}} \left(y - \sum_{r=-\infty}^{\infty} a_r\right) e^{-in\omega(t-\tau)} dt = \frac{\Delta_n}{\kappa_n}, \quad n = m, \tag{2}$$

$$\int_{\tau}^{\tau+\frac{2\pi}{\omega}} a_n e^{-im\omega(t-\tau)} dt = \frac{\Delta_n - \frac{\kappa_n}{\kappa_m}\Delta_m}{i(n-m)\omega}, \quad n \neq m, \tag{3}$$

where $n \in \mathbb{Z}$, $m \in \mathbb{Z}$, and $\Delta_n = a_n(\tau + \frac{2\pi}{\omega}) - a_n(\tau)$. Δ_n denotes the deviation of the final state of a_n from its initial state in the designated interval. The necessary condition for the synchronized system to be periodic with frequency ω is described by $\Delta_n = 0$. Equations (2) and (3) reveal that $\Delta_n = 0$ describes the sufficient condition as well. Under this condition, Eq. (2) implies that the coupling signal is identically zero in the entire interval yielding $y = \sum_{r=-\infty}^{\infty} a_r$, while Eq. (3) reveals that a_n has a single component of frequency $n\omega$. In other words, the synchronized system exhibits a periodic behavior with frequency ω, whose n^{th} component is identical to the n^{th} term in the Fourier expansion of y, if and only if, $\Delta_n = 0$ for $n \in \mathbb{Z}$. This criterion allows identification of unstable orbits embedded in the chaotic signal y by examining the periodicity of the well-defined system of Eq. (1).

An alternative way of examining this criterion is to study the behavior of the coupling signal. Referring to Eq. (2), the power of the coupling signal $f(\tau,\omega)$ in the designated interval can be expressed by

$$\langle f(\tau,\omega)\rangle = \sum_{n=-\infty}^{\infty} \left| \frac{a_n\left(\tau + \frac{2\pi}{\omega}\right) - a_n(\tau)}{\frac{2\pi}{\omega}\kappa_n} \right|^2, \tag{4}$$

which reflects the deviation of the system from a periodic orbit. This paper investigates the behavior of $\langle f(\tau,\omega)\rangle$ to detect UPOs embedded in the chaotic signal y. It utilizes the fact that a typical chaotic trajectory visits the small neighborhood of each unstable orbit during its temporal evolution on the attractor. It approaches an unstable orbit along the stable manifold, smears out the orbit for *a priori* unknown period of time, and leaves the orbit along its unstable manifold to some other orbits embedded in the attractor. Suppose that the system evolves close to an unstable orbit with frequency ω_o in the interval $\tau_o < t < \tau_o + \frac{2\pi}{\omega}$. In this situation, y exhibits a periodic behavior, which can be described by

$$y = \sum_{m=-\infty}^{\infty} y_m e^{im\omega_o t}. \tag{5}$$

This paper intends to identify τ_o, ω_o, and y_m by investigating the behavior of $f(\tau,\omega)$, as the system evolves on the chaotic attractor. Solving Eq. (1) on the target UPO yields an explicit expression for the coupling signal as

$$f(\tau_o,\omega) = \sum_{m=-\infty}^{\infty} \left(1 + \sum_{n=-\infty}^{\infty} \frac{\kappa_n}{im\omega_o - in\omega}\right)^{-1} y_m e^{im\omega_o t}. \tag{6}$$

Equation (6) reveals that the intensity of the components of the coupling signal exhibit notches that drop to zero at integer submultiples of ω_o. The coupling signal exhibits a similar behavior as $\tau \to \tau_o$ for $\omega = \omega_o$. The fact that the frequency of periodic oscillations dependent on the amplitude in nonlinear systems, allows expressing the coupling signal at the vicinity of the unstable orbit as

$$f(\tau,\omega_o) = \sum_{m=-\infty}^{\infty} \left(1 + \sum_{n=-\infty}^{\infty} \frac{\kappa_n}{im\tilde{\omega} - in\omega_o}\right)^{-1} \tilde{y}_m e^{im\tilde{\omega}t}, \tag{7}$$

where $\tilde{\omega}$ and $\tilde{y}_m$ converge to ω_o and y_m as the system approaches the unstable orbit along the stable manifold, and diverge from those values, as it leaves the orbit along the unstable manifold. In other words, the power of the coupling signal exhibits a notch that drops to zero at $\tau = \tau_o$. Equations (6) and (7) show that ω_o and τ_o can be identified at notches of $\langle f(\tau,\omega)\rangle$, while y_m is determined by the amplitude of a_m in the designated interval.

This paper suggests investigating a time average of $\langle f(\tau,\omega)\rangle$ over the entire time series as described by

$$\bar{f}(\omega) = \frac{\int w(\tau,\omega)\langle f(\tau,\omega)\rangle d\tau}{\int w(\tau,\omega) d\tau}, \tag{8}$$

where $w(\tau,\omega) = \langle f(\tau,\omega)\rangle^{-\alpha}$ for $\alpha \geqslant 0$. The weight function $w(\tau,\omega)$ is assigned based on the fact that the power of the coupling signal is more important around $\tau = \tau_o$ than other regions, when detecting UPOs is concerned. ω_o can be extracted at notches of $\bar{f}(\omega)$, and τ_o can be identified at the notch shape minima of $f(\tau,\omega_o)$. Once ω_o and τ_o are extracted, the components of the unstable orbit can be evaluated by

$$y_n = \frac{\omega_o}{2\pi}\int_{t=\tau_o}^{\tau_o+\frac{2\pi}{\omega_o}} a_n(t)e^{-in\omega_o t}dt. \tag{9}$$

The proposed theoretical procedure can be implemented in practical situations, where y is only available at discrete time points $\{t_1,t_2,\ldots,t_J\}$ as a finite sequence of samples $\{y_1,y_2,\ldots,y_J\}$. Note that the magnitude of a_n vanishes exponentially with respect to n, once the system starts evolving close to a periodic orbit. This suggests employing a truncated version of the synchronized system, for which the components with $|n| > N$ are assumed to have negligible contributions to the response of the system. The truncated version of Eq. (1) can be solved for a_n at each consecutive sampling time using the Euler exponential integrator [13] over a desirable set of discrete frequencies $\{\omega_1,\omega_2,\ldots,\omega_K\}$ defined by

$$\omega_k = \frac{1}{L_k}\frac{2\pi}{\Delta t}, \tag{10}$$

where Δt is the sampling period, and L_k is the number of samples in the designated interval. The following outlines the steps involved in the implementation of the proposed methods starting with $k = 1$ and $j = 1$.

(1) Numerical integration of the synchronized system for $\omega = \omega_k$ using the Euler exponential integrator that yields [13]

$$a(t_{j+1}) = e^{\Omega\Delta t}a(t_j) + \Omega^{-1}(e^{\Omega\Delta t} - I)\kappa y(t_j) \tag{11}$$

for $j = 1,2,\ldots,J-1$. In this equation, $a = [a_{-N},\ldots,a_0,\ldots,a_N]^\top$, Ω is the coefficient matrix of a in Eq. (1), and $\kappa = [\kappa_{-N},\ldots,\kappa_0,\ldots,\kappa_N]^\top$, where the superscript $\top$ denotes the transpose of a matrix. Note that $e^{\Omega\Delta t}$ and $\Omega^{-1}(e^{\Omega\Delta t} - I)\kappa$ are constant matrices that are evaluated once for the whole integration process. The initial condition required for the integration is arbitrary, as the results are derived independently from the initial conditions.

(2) Evaluation of the power of the coupling signal at each time point τ_j for $j \leqslant J - L_k$ according to

$$\langle f(\tau_j,\omega_k)\rangle = \sum_{n=-N}^{N}\left|\frac{a_n\left(\tau_j + \frac{2\pi}{\omega_k}\right) - a_n(\tau_j)}{\frac{2\pi}{\omega_k}\kappa_n}\right|^2. \tag{12}$$

(3) Evaluation of the weighted time average of of the power of the coupling signal over the entire time series. Equation (13) allows evaluating $\bar{f}(\omega)$ for a given α as

$$\bar{f}(\omega_k) = \frac{\sum_{j=1}^{J-L_k}\langle f(\tau_j,\omega_k)\rangle^{1-\alpha}}{\sum_{j=1}^{J-L_k}\langle f(\tau_j,\omega_k)\rangle^{-\alpha}}. \tag{13}$$

(4) $k \to k+1$ and return to step 1, if $k < K$.

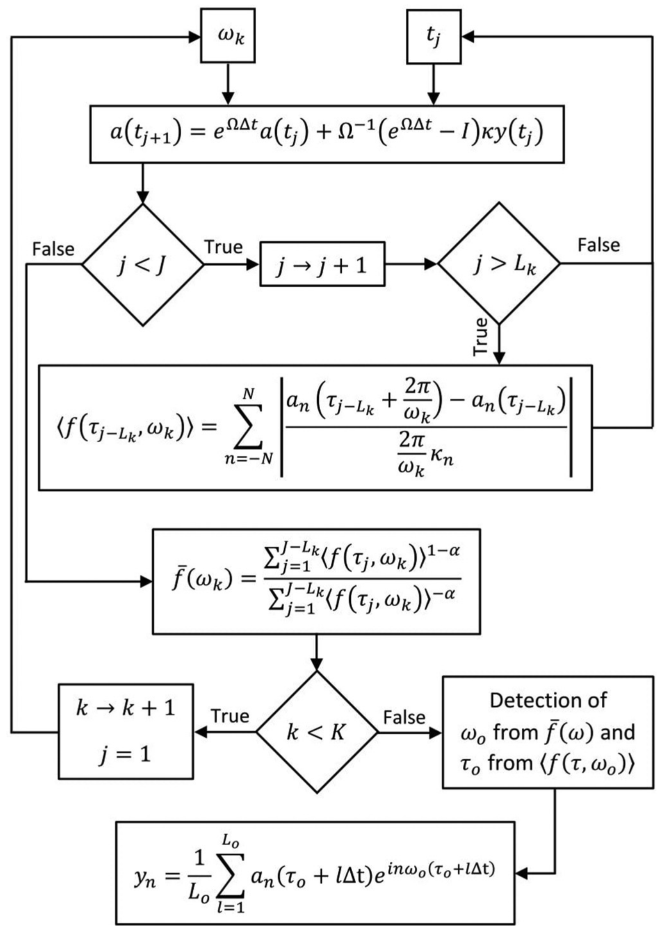

FIG. 1. Flow chart of detecting UPOs in chaotic time series.

(5) Evaluation of the components of the periodic orbit according to

$$y_n = \frac{1}{L_o}\sum_{l=1}^{L_o} a_n(\tau_o + l\Delta t)e^{-in\omega_o(\tau_o+l\Delta t)}, \tag{14}$$

where ω_o and τ_o are identified at notches of $\bar{f}(\omega)$ and $\langle f(\tau,\omega_o)\rangle$, respectively, and L_o is the number of samples in the interval $\tau_o \leqslant t \leqslant \tau_o + \frac{2\pi}{\omega_o}$.

Figure 1 presents a schematic of the proposed algorithm of detecting UPOs in chaotic time series.

III. RESULTS AND DISCUSSIONS

To demonstrate the capabilities of the proposed approach, detecting UPOs embedded in chaotic attractors of the Rössler system and Mackey-Glass equation for a simple coupling condition of $\kappa_n = \frac{\omega}{\pi}$ is addressed.

A. Rössler System

The well-known Rössler system can be defined by the following system of differential equations:

$$\begin{bmatrix}\dot{x}_1\\ \dot{x}_2\\ \dot{x}_3\end{bmatrix} = \begin{bmatrix}-x_2 - x_3\\ x_1 + 0.2x_2\\ 0.2 + x_3(x_1 - 5.7)\end{bmatrix}. \tag{15}$$

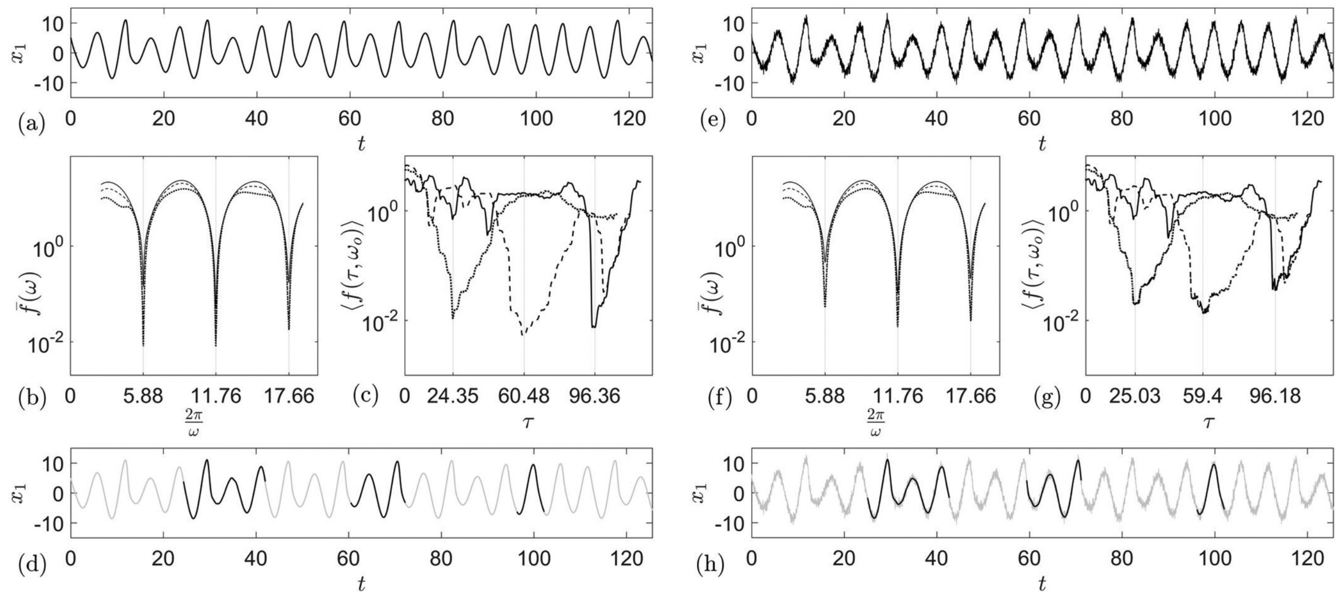

FIG. 2. Extracting the coordinates of UPOs from the x_1 component of the Rössler system. (i) Noise-free data: (a) the recorded time history, (b) the time average of the coupling signal for $\alpha = 0$ (—), $\alpha = 1$ (− − −), $\alpha = 2$ (· · · ·), (c) the power of the coupling signal for period-1 orbit (solid line), period-2 (dashed line), period-3 (dotted line), (d) the extracted component of the periodic evolution. (ii) White Gaussian noise contaminated data with signal-to-noise ratio of 1dB: (e) the recorded time history, (f) the time average of the coupling signal for $\alpha = 0$ (solid line), $\alpha = 1$ (dashed line), $\alpha = 2$ (dotted line), (g) the power of the coupling signal for period-1 orbit (solid line), period-2 (dashed line), period-3 (dotted line), (h) the extracted component of the periodic evolution.

Assume that the x_1 component of the system is available for measurement. Figure 2 plots the results obtained from the recorded time history of 5000 samples with the sampling rate 40 Sps. The first set of results is presented for a noise-free time series as plotted in Fig. 2(a) for $N = 12$. The period of UPOs embedded in the measured signal is identified at notches of $\bar{f}(\omega)$, as illustrated in Fig. 2(b). Figure 2(c) plots the power of the coupling signal at the extracted frequencies. τ_o is identified at the notch shape minima of $\langle f(\tau,\omega_o)\rangle$. Extracting ω_o and τ_o allows evaluating the x_1 component of the periodic orbit through Eq. (14) as plotted in Fig. 2(d). Note that the notches of Fig. 2(b) are very close to the first, second, and third multiples of $\frac{2\pi}{\omega} = 5.88s$. This implies the notches of this figure may correspond to a single UPO around which the system evolves for one, two, and three times of the period of the UPO. To refute this possibility in the frequency domain, the power of the coupling signal at each frequency needs to be analyzed in the time domain. As illustrated in Fig. 2(c), the notch shape minima of the power of the coupling signal at the detected frequencies are separated by several periods of the UPO, and no overlap is observed. This indicates the notches of Fig. 2(b) correspond to distinct UPOs as illustrated in Fig. 2(d). Figure 2(e) plots the white Gaussian noise contaminated signal with signal-to-noise ratio (SNR) of 1 dB. Following the same steps leads to the results which agree with those obtained from the noise-free signal. Comparing Figs. 2(b) and 2(f) reveals that noise has minimum effects on the identification of ω_o. This is important form a practical point of view, as the fundamental frequency of unstable orbits is a critical piece of information in many chaos control techniques [13,14]. Comparing Figs. 2(c) and 2(g) indicates that the presence of noise has a negligible effect on detection of τ_o. Figure 2(h) reveals that noise has also slight effects on extraction of the frequency components of the unstable orbit, due to the filtering properties of Eq. (14). In fact, this equation reduces the effect of noise by filtering out the undesirable frequencies from the components of the synchronized system. In contrast to noise-free data, Eq. (14) reveals that a larger truncation limit N does not necessarily lead to a more accurate result, as the higher order components capture the effect of noise in distorting the signal rather than improve the quality of the results. In practice, an optimal value of N is a limit beyond which the depth of the notches stops following a descending pattern as the truncation limit increases. Following this criterion leads to $N = 9$ for the noisy time series. The results presented in Fig. 2 agree with those reported in the literature [16].

To evaluate the accuracy of the results, the detected orbits are used to control chaotic behavior of the system using the classical proportional feedback controller [17]. Note that the intensity of the error signal in the feedback loop reflects the quality of the extracted orbits. Figure 3 plots the error signal in the control process of periodic orbit of period $\frac{2\pi}{\omega} = 11.76s$. As illustrated in Fig. 3(a), the noise-free data leads to a practically vanishing error reflecting the accuracy of the extracted orbit. Figure 3(b) shows that the noise contaminated data leads to small oscillations of the error around zero. It indicates slight deviations of the extracted orbit from the UPO embedded in the attractor. Figure 4 illustrates the dependence of the error in the control process to the level of the noise in the time series for $N = 9$. It plots the root mean square of the error over one period of the target orbit E_{RMS} for different signal-to-noise ratios (SNR). The random nature of the noise leads to slightly different time series even for the same level of noise. The results presented in Fig. 4 are obtained based

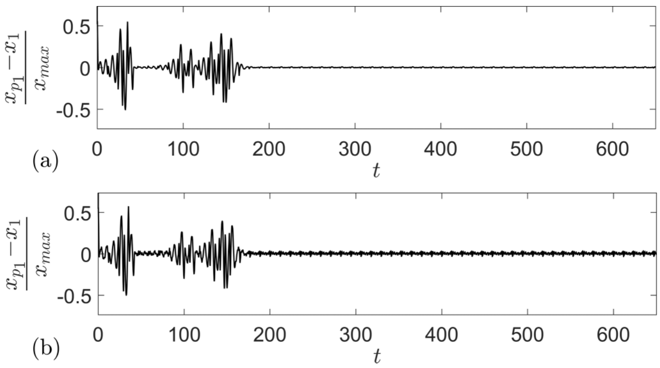

FIG. 3. The error signal obtained from (a) noise-free data and (b) noisy data. $x_{\max}$ denotes the maximum of x_{p_1} in one period of the detected orbit. The control is switched on at $t = 150$, and is applied to the first component of the vector field through the feedback $\kappa_p(x_{p_1} - x_1)$ of gain $\kappa_p = 0.5$.

on the average of E_{RMS} for 10 noisy time series with the same signal-to-noise ratio. It shows that the detected orbit in Gaussian white noise contaminated data approaches to the orbit detected in the noise free data as the signal-to-noise ratio increases.

B. Mackey-Glass equation

The Mackey-Glass equation has been known as a paradigmatic model for studying high-dimensional chaos, which can be described by the following functional differential equation:

$$\dot{x} = \frac{2x(t-2)}{1 + x(t-2)^{9.65}} - x. \tag{16}$$

This system exhibits a chaotic behavior for the parameters of Eq. (16). The dynamics of this time delay system takes place in an infinite dimensional function space, which makes identification of the UPOs embedded in its chaotic attractor particularly challenging. The results of this section show that the proposed method of this paper can accurately detect UPOs in time series of such a high-dimensional system.

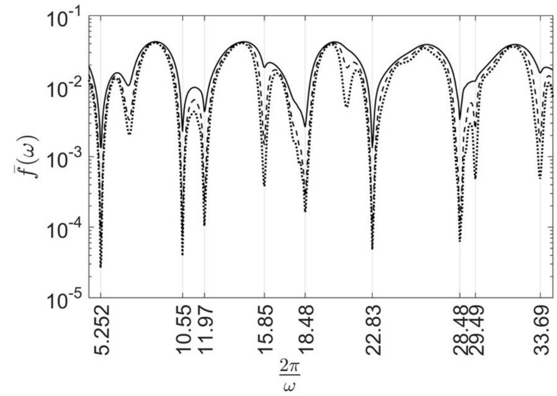

FIG. 5. Detecting the periods of UPOs from the $x(t)$ component of the Mackey-Glass equation for $\alpha = 0$ (solid line), $\alpha = 1$ (dashed line), and $\alpha = 2$ (dotted line).

Figure 5 plots $\bar{f}(\omega)$ obtained from the $x(t)$ component of the system for $N = 20$. A time series of 30 000 data points sampled at 20 Sps is processed. Nine notches can be identified clearly in the desirable range of frequency, each of which may correspond to a distinct UPO. It can be observed that the first, second, and fourth notches of Fig. 5 are very close to the first, second, and third multiples of $\frac{2\pi}{\omega} = 5.252s$. This suggests that they may correspond to a single UPO of period $\frac{2\pi}{\omega} = 5.252s$, around which the chaotic trajectory spends one, two, and three times of this period, respectively. To verify the validity of this possibility, the power of the coupling signal at each frequency needs to be analyzed in the time domain. Figure 6 plots the power of the coupling signal at the detected frequencies. The separation between the minima in each case is smaller that the period $\frac{2\pi}{\omega} = 5.252s$. This result reveals that all the three notches belong to a single UPO of period $\frac{2\pi}{\omega} = 5.252s$. Note that a similar condition is observed throughout the entire time series when this UPO is detected. It can be verified that

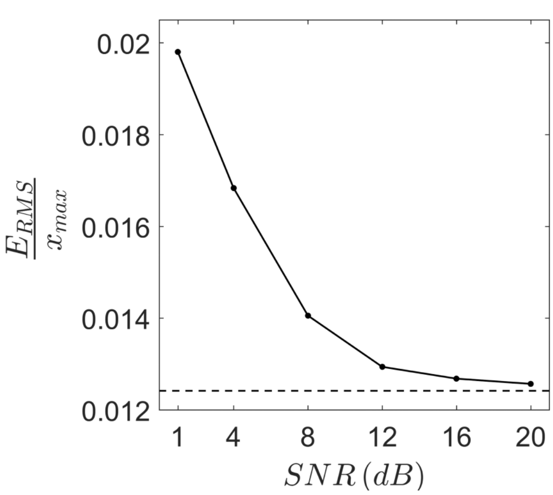

FIG. 4. Dependence of the root mean square of the error in the control loop to the level of noise for $N = 9$. The dashed line indicates the error associated with the noise free data.

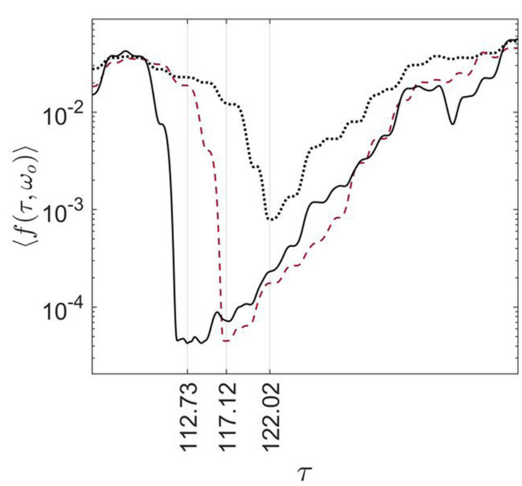

FIG. 6. Power of the coupling signal for $\frac{2\pi}{\omega} = 5.25s$ (solid line), $\frac{2\pi}{\omega} = 10.55s$ (dashed line), and $\frac{2\pi}{\omega} = 15.85s$ (dotted line).

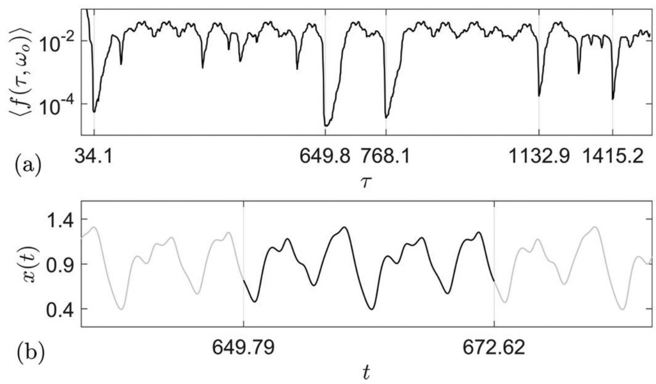

FIG. 7. Detecting UPO of period $\frac{2\pi}{\omega} = 22.83s$ from the $x(t)$ component of the Mackey-Glass equation (a) power of the coupling signal and (b) detected periodic motion.

the remaining notches correspond to distinct UPOs embedded in the chaotic attractor.

Once the periods of UPOs are extracted, the moment at which the system starts approaching to an unstable orbit can be detected at the notches of the power of the coupling signal. Figure 7 illustrates the result of detecting periodic orbits of period $\frac{2\pi}{\omega_o} = 22.83s$. Figure 7(a) shows that the system visits this periodic orbit several times during its temporal evolution on the attractor. The unstable orbit can be identified best at $t = 649.79s$, as the power of the coupling signal has a lower minimum. Figure 7(b) plots the $x(t)$ component of the detected orbit. Following a similar approach allows detecting the rest of the UPOs that correspond to the notches of Fig. 5, as plotted in Fig. 8. The orbits presented with dots correspond to the controlled orbit through the proportional feedback controller. Small deviations of the controlled orbit from the detected one indicate the capabilities of the proposed method in extracting UPOs from time series of high-dimensional chaotic systems.

IV. CONCLUSION

This paper utilizes the concept of synchronization to develop a method of detecting UPOs embedded in chaotic times series. It reveals that UPOs can be detected at the intervals in which the power of the coupling drops towards zero in the form of a notch. The depth of the notch reflects the deviation of the chaotic trajectory from the unstable orbit. In this paper, the dominant notch with the lowest minimum is used to extract the coordinates of the UPO. The current scheme can be extended to incorporate the information from several notches emerging from frequent visits of the chaotic trajectory and the UPO to improve the quality of the detected orbit. The proposed approach detects UPOs using a single state of the system under a simple coupling condition. Therefore, it is appealing in experimental situations. When the real time detection of UPOs is concerned, the simple and efficient integration algorithm described by Eq. (11) can be used in real time implementation of the proposed method using digital computers [13]. To do so, the frequency of the target orbit needs to be extracted first using a recoded time history of the system by following steps 1–4 of the proposed algorithm. Note that this step can be avoided when dealing with nonautonomous systems as the frequency of the UPOs are explicitly known as integer submultiples of the frequency of the external force. An alternative approach is to build a set of linear oscillators using electrical components for each extracted frequency to facilitate real time detection of the target UPOs in fast chaotic systems. The application of this method can be extended to analyze the behavior of chaotic systems, as the underlying dynamics is characterized by the set of UPOs embedded in the chaotic attractor.

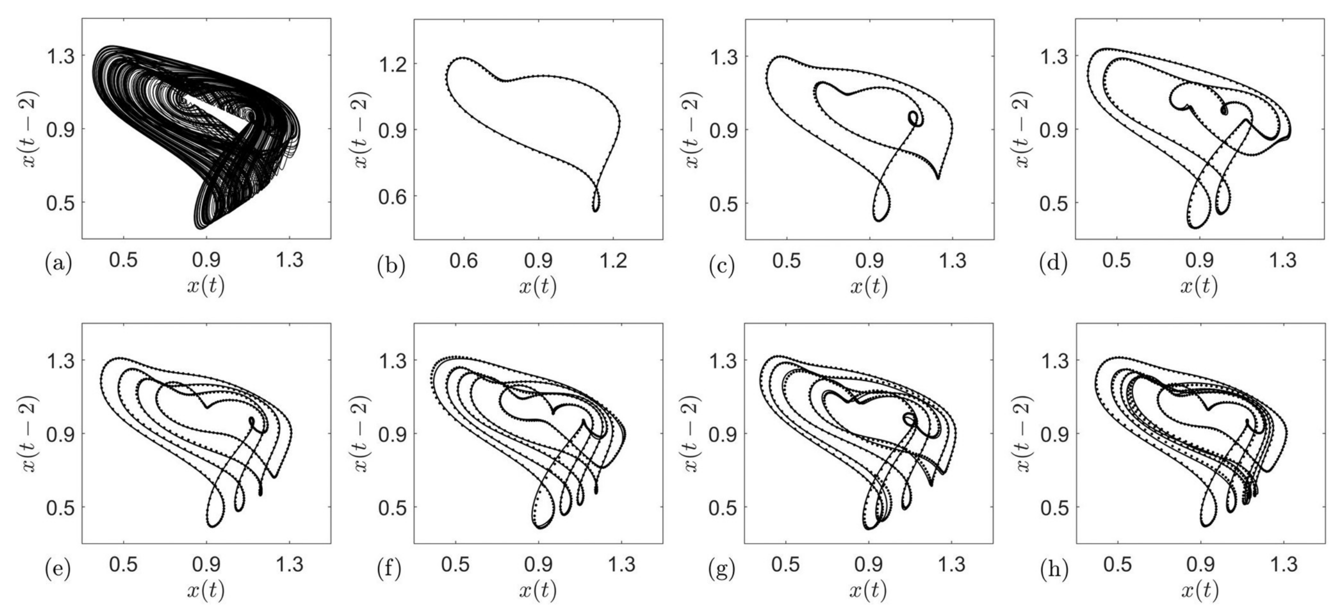

FIG. 8. Two-dimensional projection of (a) chaotic attractor, detected UPOs (solid line), and controlled orbit (dotted line) of the Mackey-Glass equation with periods (b) $\frac{2\pi}{\omega_o} = 5.255s$, (c) $\frac{2\pi}{\omega_o} = 11.97s$, (d) $\frac{2\pi}{\omega_o} = 18.48s$, (e) $\frac{2\pi}{\omega_o} = 22.83s$, (f) $\frac{2\pi}{\omega_o} = 28.48$, (g) $\frac{2\pi}{\omega_o} = 29.49s$, and (h) $\frac{2\pi}{\omega_o} = 33.69s$. The control is applied through the feedback $\kappa_p(x_p - x)$ of gain $\kappa_p = 1.5$.

[1] D. Auerbach, P. Cvitanovic, J. P. Eckmann, G. Gunaratne, and I. Procaccia, Phys. Rev. Lett. **58**, 2387 (1987).
[2] T. L. Carroll, Phys. Rev. E. **59**, 1615 (1999).
[3] E. Ott, C. Grebogi, and J. A. Yorke, Phys. Rev. Lett. **64**, 1196 (1990).
[4] S. Hayes, C. Grebogi, E. Ott, and A. Mark, Phys. Rev. Lett. **73**, 1781 (1994).
[5] B. Kia, A. Dari, W. L. Ditto, and M. L. Spano, Chaos **21**, 047520 (2011).
[6] D. P. Lathrop and E. J. Kostelich, Phys. Rev. A **40**, 4028 (1989).
[7] P. So, E. Ott, S. J. Schiff, D. T. Kaplan, T. Sauer, and C. Grebogi, Phys. Rev. Lett. **76**, 4705 (1996); P. So, E. Ott, T. Sauer, B. J. Gluckman, C. Grebogi, and S. J. Schiff, Phys. Rev. E **55**, 5398 (1997).
[8] H. Ma, W. Lin, and Y. C. Lai, Phys. Rev. E **87**, 050901(R) (2013).
[9] Z. Gao and N. Jin, Nonlinear Anal. Real. **13**, 947 (2012).
[10] D. Walker and M. Small, IEEE Trans. Circuits Syst. I **53**, 2818 (2006).
[11] M. Buhl and M. Kennel, Chaos **17**, 033102 (2007).
[12] F. Takens, in *Dynamical Systems and Turbulence*, edited by D. Rand and L. S. Young, Lecture Notes in Mathematics Vol. 898 (Springer-Verlag, Berlin, 1981), p. 366.
[13] A. A. Olyaei and C. Wu, Phys. Rev. E **91**, 012920 (2015).
[14] J. E. S. Socolar, D. W. Sukow, and D. J. Gauthier, Phys. Rev. E **50**, 3245 (1994).
[15] V. Pyragas and K. Pyragas, Phys. Rev. E **92**, 022925 (2015).
[16] G. Chen and X. Yu, IEEE Trans. Circuits Syst. I, Fundam. Theory **46**, 767 (1999); V. Pyragas and K. Pyragas, Phys. Lett. A **375**, 3866 (2011).
[17] K. Pyragas, Phys. Lett. A **170**, 421 (1992).